Natural Convection Heat Transfer Enhancement in a Differentially Heated parallelogrammic Enclosure Filled with Cooper-Water Nanofluid

Salam Hadi Hussain
Babylon University/ College of Engineering

Abstract

Laminar steady natural convection of a nanofluid consists of water and copper in a differentially heated parallelogrammic enclosure has been studied and solved numerically using finite volume method. Two-dimensional governing equations have been solved to investigate the flow behavior over a wide range of the Rayleigh numbers ($10^4 \leq Ra \leq 10^6$), skew angles ($-60° \leq \Phi \leq +60°$), aspect geometric ratios ($0.5 \leq AR \leq 4$) and solid volume fractions ($0 \leq \varphi \leq 0.2$). Effects of all these parameters on the flow and thermal fields are presented in the form of streamline, isotherm contours and average Nusselt number and discussed in detail. It is shown that the heat transfer rate increases remarkably by the addition of copper-water nanofluid and the shape of the convection vortices is sensitive to the skew angle variation. Also, it is observed that the average Nusselt number at the hot left sidewall increases with the increasing of the solid volume fraction and the Rayleigh number. Comparison with previous published work on the natural convection in a nanofluid filled enclosure is performed and an excellent agreement between the results is observed.

Keywords: Nanofluid, natural convection, aspect ratio, parallelogrammic enclosure, copper-water, finite volume.

الخلاصة

تم في هذا البحث دراسة الحمل الحراري الحر والطباقي والمستقر لمائع نانوي مؤلف من الماء وذرات متناهية الصغر ونانوية من النحاس داخل فجوة او حيز مغلق متفاضل التسخين عددياً وباستخدام طريقة الحجوم المحددة (finite volume method). المعادلات الثنائية البعد الحاكمة تم حلها لتقصي سلوك وطبيعة الجريان لأرقام مختلفة من اعداد رالي ($10^4 \leq$ Ra $\leq 10^6$) ، زاوية الانحدار للجدارين الجانبيين ($-60° \leq \Phi \leq +60°$)، نسبة المساحة ($0.5 \leq$ AR≤ 4) ونسب الحيود للذرات الصلبة ($0 \leq \varphi \leq 0.2$). ان التأثيرات المختلفة لكل هذه المتغيرات المدروسة تم تمثيلها بدلالة خطوط دالة الانسياب ودرجات الحرارة واعداد نسلت المتوسطة كما تم مناقشتها بالتفصيل في هذه الدراسة. بينت نتائج هذه الدراسة ان معدل انتقال الحرارة يزداد بصورة ملحوظة بإضافة ذرات النحاس النانوية للماء كما ان شكل الدوامات المتولدة داخل الفجوة يتأثر بتغير زاوية الانحدار للجدارين الجانبيين. كما تمت ملاحظة ان قيم ارقام اعداد نسلت المتوسطة على الجدار الايسر الساخن تزداد بزيادة قيم ارقام اعداد رالي ونسبة الحيود للذرات الصلبة للنحاس. تمت مقارنة دقة نتائج البحث الحالي مع نتائج باحث اخر منشورة وتم الحصول على تطابق ممتاز في النتائج.

Nomenclature

Symbol	Description	Unit
AR	Aspect ratio (H/W)	
c_p	Specific heat at constant pressure	kJ/kg. K
g	Gravitational acceleration	m/s^2
H	Height of the parallelogrammic cavity	m
k	Thermal conductivity of fluid	$W/m.K$
$\underline{n}$	Outward flux normal to boundary	
$\overline{Nu}$	Average Nusselt number	
P	Dimensionless pressure	
p	Pressure	N/m^2
Pr	Prandtl number	
Ra	Rayleigh number	
T	Temperature	K
T_C	Temperature of the cold surface	K
T_H	Temperature of the hot surface	K
U	Dimensionless velocity component in x-direction	
u	Velocity component in x-direction	m/s
V	Dimensionless velocity component in y-direction	

v	Velocity component in y-direction	*m/s*
W	Width of the parallelogrammic cavity	*m*
X	Dimensionless coordinate in horizontal direction	
x	Cartesian coordinate in horizontal direction	*m*
Y	Dimensionless coordinate in vertical direction	
y	Cartesian coordinate in vertical direction	*m*
Greek symbols		
α	Thermal diffusivity	m^2/s
β	Volumetric coefficient of thermal expansion	K^{-1}
θ	Dimensionless temperature	
Φ	Sidewall inclination angle from vertical or skew angle	*degree*
φ	Nanoparticle volume fraction	
ϑ	Kinematic viscosity of the fluid	m^2/s
Ψ	Dimensional stream function	m^2/s
ψ	Dimensionless stream function	
μ	Dynamic viscosity of the fluid	*kg.s/m*
ρ	Density	kg/m^3
Subscripts		
C	Cold	
f	Fluid (pure)	
H	Hot	
nf	Nanofluid	
s	Solid (nanoparticle)	
Abbreviations		
FVM	Finite Volume Method	
min	Minimum	

1. Introduction

Thermal fluids are very important for heat transfer in many industrial applications. Low thermal conductivity of conventional heat transfer fluids such as water, oil, and ethylene glycol mixture is a serious limitation in improving the performance of these industrial applications. To overcome this disadvantage, there is a strong motivation to develop advanced heat transfer fluids with substantially higher thermal conductivity. One way is to add small solid particles with micrometer or even millimeter dimensions in the fluid which is called nanofluids (Akbari *et al*., 2008). Nanofluid is a suspension of solid–liquid mixture nanoparticles (1–100 nm diameter) in a traditional liquids. Sometimes, it is defined as a colloid composed of nanoparticles in a base fluid, which has been proposed as a highly-effective heat transfer medium in view of its abnormally higher thermal conductivity. Depending on size, shape, and the solid nanoparticles thermal properties, the thermal conductivity can be increased by about 40% with low concentration (1–5 % by volume) of solid nanoparticle in the mixture. The nanofluid is stable, introduce very small pressure drop and it can pass through nanochannels. Sometimes stabilizer (e.g., oleic acid and laurate salt) is added with the nanofluid to stabilize the solid particles in the mixture (Santra *et al*., 2009 and Anoop *et al*., 2009).With the development of material science and modern techniques of producing nano-sized particles, more attention has been devoted in suspending these nano-sized particles (nanofluids) in a base fluid. Nanofluids are utilized in numerous biological, and scientific applications, such as blood clogging, cell transport in arteries and veins, drug and gene delivery and manufacturing of nanocomposites because the presence of the nanoparticles in the fluids increases their effective thermal conductivities and consequently enhances their heat transfer characteristics (Elgafy and Lafdi, 2007). Moreover, nanofluids have a wide range of significant applications like electronics, automotive and nuclear applications where improved heat transfer or efficient heat dissipation is required. In the literature, various research works have been focused mainly on identifying and modeling the natural convection in enclosure filled with nanofluid. Keblinski *et al*. (2002) studied mechanisms of heat flow in suspensions of nano-sized particles.They demonstrated that the thermal conductivity increased of nanofluids due to Brownian motion of particles, molecular-level layering of the liquid at the liquid-particle interface, the nature of heat transport in the nano particles and the effect of nano particle clustering. Khanafer *et al*. (2003) studied buoyancy-driven heat transfer enhancement numerically in a two-dimensional rectangular enclosure containing nanofluids. The nanofluid in the enclosure was assumed to be in a single phase. They used Brinkman model and Wasp's model for nanofluid viscosity and thermal conductivity respectively. The results indicated that at any fixed Grashof number, the nanofluid heat transfer rate increased with an increase in the nano particle volume fraction. Jou and Tzeng (2006) simulated numerically natural convection heat transfer of copper-water nanofluids in a two dimensional rectangular enclosure. They reported an increase in the heat transfer by the addition of nanoparticles. Ho and Lin (2006) studied experimentally natural convection heat transfer in a vertical square enclosure filled with Al_2O_3-water nanofluid of different mass fraction. They observed a substantial heat transfer reduction except the cases of the particle mass fraction not higher than 1% wt. Hwang *et al*. (2007) investigated theoretically the heat transfer characteristics of natural convection in a rectangular cavity heated from below. Nanoparticles of Al_2O_3 were suspended in water. They concluded that the ratio of heat transfer coefficient of nanofluids to that of base fluid was decreased as the size of nanoparticles increased, or the average temperature of nanofluids was decreased. Trisaksri and Wongwises (2007) and Wang and Mujumdar (2007) conducted a literature review on the general heat transfer characteristics of nanofluids. While Daungthongsuk and Wongwises (2007) performed a comprehensive review of convective heat transfer phenomenon for nanofluids. Ho *et al*. (2008) presented a numerical identification for the effects due to uncertainties in effective dynamic viscosity and thermal conductivity of nanofluid on laminar natural convection heat transfer in a square enclosure with alumina–water nanofluid. They found that the significant difference in the effective dynamic viscosity enhancement of the nanofluid played a major role and led to contradictory results concerning the heat transfer efficiency of using nanofluid in the enclosure. Santra *et al*. (2008) numerically investigated the laminar natural convection heat transfer in a differentially heated square cavity filled with copper-water nanofluid. They considered a two parameter power law model for an incompressible non-Newtonian fluid. Oztop and Abu-Nada (2008) simulated numerically heat transfer and fluid flow due to buoyancy forces in a partially heated rectangular enclosure using nanofluids with different types of nanoparticles. The flush mounted heater was located to the left vertical wall with a finite length. The temperature of the right vertical wall was lower than that of heater while the other walls were considered insulated. The finite volume technique was used to solve the governing equations. It was found that the heater location affected the flow and temperature fields when using nanofluids. Also, the heat transfer enhancement using nanofluids was more pronounced at low aspect ratio than at high aspect ratio. Anilkumar and Jilani (2009) investigated numerically single phase natural convective heat transfer in an enclosure with fin utilizing nanofluids. The nanofluid used, which was composed of Aluminum oxide nano particles in suspension of Ethylene glycol which was provided at various volume fractions. The study was carried out for a different range of Rayleigh numbers, fin heights and aspect ratios. The results illustrated that the nanofluid heat transfer rate increased with an increase in the nano particles volume fraction. Also they found that, the presence of nano particles in the fluid altered the structure of the fluid flow. Ghasemi and Aminossadati (2009) presented the results of a numerical study on natural convection heat transfer in an inclined enclosure filled with a water-CuO nanofluid. Two opposite walls of the enclosure were insulated and the other two walls were kept at different temperatures. The transport equations for a Newtonian fluid were solved numerically with a finite volume approach using the SIMPLE algorithm. The influence of pertinent parameters such as Rayleigh number, inclination angle and solid volume fraction on the heat transfer characteristics of natural convection was studied. The results indicated that adding nanoparticles into pure water improved its heat transfer performance; however, there was an optimum solid volume fraction which maximized the heat transfer rate. The results also showed that the inclination angle had a significant impact on the flow and temperature fields and the heat transfer performance at high Rayleigh numbers. Aminossadati and Ghasemi

(2009) investigated natural convection cooling of a localized heat source at the bottom of a nanofluid-filled enclosure. They found that adding nanoparticles into pure water improved its cooling performance especially at low Rayleigh numbers. Ho *et al*. (2010) investigated experimentally the natural convection heat transfer of Al_2O_3-water nanofluid in vertical square enclosures of three different sizes together with measurements for the thermophysical properties of the nanofluids. A correlation analysis based on the thermophysical properties for the nanofluids formulated showed that the heat transfer efficiency of using nanofluid for natural convection in enclosure was dependent on the net influences by the relative changes in the thermophysical properties of the nanofluid with respect to its base fluid. Ghasemi and Aminossadati (2010) studied numerically the natural convection cooling of an oscillating heat source embedded on the left wall of a square enclosure filled with nanofluids. The effects of various important parameters such Rayleigh number, solid volume fraction, heat source position, type of nanofluid and oscillation period on the cooling performance of the enclosure were examined. They concluded that the utilization of nanoparticles, in particular Cu, enhanced the heat transfer especially at low Rayleigh numbers. In addition, the oscillation period of heat generation affected the maximum operational temperature of the heat source. Abu-Nada *et al*. (2010) investigated the heat transfer enhancement in a differentially heated enclosure using variable thermal conductivity and variable viscosity of Al_2O_3-water and CuO-water nanofluids. The results were presented over a wide range of Rayleigh numbers, volume fractions of nanoparticles and aspect ratios. It was observed that enclosures, having high aspect ratios, explained more deterioration in the average Nusselt number when compared to enclosures having low aspect ratios. Also, it was found that at high Rayleigh numbers the average Nusselt number was more sensitive to the viscosity models than to the thermal conductivity models. Corcione (2010) investigated theoretically the heat transfer features of buoyancy-driven nanofluids inside rectangular enclosures differentially heated at the vertical walls. The heat transfer enhancement across the differentially heated enclosure that derived from the dispersion of nano-sized solid particles into a host liquid was calculated for different operating conditions, nanoparticle diameters, combinations of suspended nanoparticles and base liquid and cavity aspect ratios. He concluded that the optimal volume fraction was found to increase slightly with decreasing the nanoparticle size. Lin and Violi (2010) analyzed the heat transfer and fluid flow of natural convection in a vertical cavity filled with Al_2O_3-water nanofluid that operated under differentially heated walls. The heat transfer rates were examined for parameters of non-uniform nanoparticle size, mean nanoparticle diameter, nanoparticle volume fraction, Prandtl number, and Grashof number. They concluded that by decreasing the Prandtl number resulted amplifying the effects of nanoparticles due to increase the effective thermal diffusivity. Alloui *et al*. (2012) reported an analytical and numerical study of natural convection in a shallow rectangular cavity filled with nanofluids. Neumann boundary conditions for temperature were applied to the horizontal walls of the enclosure, while the two vertical ones were assumed insulated. The problem governing parameters were the Rayleigh number, the Prandtl number, and the aspect ratio of the cavity and the solid volume fraction of nanoparticles. It was found that the presence of nanoparticles in a fluid reduced the strength of flow field and this behaviour being more pronounced at low Rayleigh number. Also, the temperatures on the solid boundaries were reduced (enhanced) by the presence of the nanoparticles when the strength of convection was high (low). Mahmoudi *et al*. (2010) presented a numerical study of natural convection cooling of a heat source horizontally attached to the left vertical wall of a square cavity filled with copper-water nanofluid. The left vertical wall was kept at the constant temperature, while the other ones were kept adiabatic. The numerical approach was based on the finite volume method with a collocated grid arrangement. It was observed that at a given Rayleigh number and definite heat source geometry, the average Nusselt number increased linearly with the increase in the solid volume fraction of nanofluid. From the other side, various research papers are studied natural convection phenomenon in a parallelogrammic enclosure filled with different classical fluids or pure fluids (Chung and Trefethen, 1982; Maekawa and Tanasawa, 1982; Seki *et al*., 1983; Hyun and Choi, 1990; Aldridge and Yao, 2001; Baïri, 2008). In fact, for various practical applications, the parallelogrammic enclosures have a strong potential to be used in the assembly of construction elements, since they present an excellent heat transfer performance relative to the classical square or rectangular shape. Many studies (Chung and Trefethen, 1982; Maekawa and Tanasawa, 1982; Seki *et al*., 1983; Hyun and Choi, 1990; Aldridge and Yao, 2001; Baïri, 2008; Saleh *et al*., 2011) explained that the parallelogrammic enclosure can be used as a heat transfer inhibitor (thermal insulation) or act as a heat transfer promoter (heat transfer enhancement). But none of them studied this problem when the parallelogrammic enclosure is filled with cooper-water nanofluid for various aspect geometric ratios ($0.5 \leq AR \leq 4$) and high Cu concentration ratios ($0 \leq \varphi \leq 0.2$) when the sloping walls are inclined at an angle (Φ) with respect to the vertical which is varied as 0°, ± 30°, ± 60° respectively. This point represents the major original contribution of the present work. Therefore; the purpose of the present work is to examine the effects of Rayleigh number, solid volume fraction, aspect geometric ratio and skew angle on the natural convection in a two-dimensional parallelogrammic enclosure filled with Cu-water nanofluid.

2. Mathematical modeling

2.1. Geometrical configuration and governing equations

Figure 1 shows a two-dimensional parallelogrammic enclosure of length (H) and width (W).The enclosure is filled with a suspension of copper nanoparticles in water. Both the vertical left and right sidewalls are maintained at constant hot and cold temperatures respectively. In order to create the buoyancy effect, the left vertical wall is kept at a higher temperature than the right one. The parallelogrammic enclosure left and right sidewalls are inclined at an angle (Φ) with respect to the vertical (sometimes called skew angle). The other two horizontal upper and lower walls are assumed adiabatic. The Rayleigh number (Ra) varying from 10^4 to 10^6, while the solid volume fractions, (φ) have been varied from 0 % to 20 % with an increment of 5%. The skew angle is varied as 0°, -30°, -60°, 30° and 60° respectively. The enclosure aspect ratio (AR = H / W) varying from 0.5 to 4.Water has been considered as the base fluid, while copper (Cu) nanoparticles mixed with water, has been considered as nanofluid. The thermo-physical properties of base fluid (water) and copper nanoparticle are listed in Table 1.The problem is modeled mathematically based on the following assumptions:

1.The nanofluid in the enclosure is considered Newtonian, steady, laminar, and incompressible and is assumed to have uniform size and shape.
2. Both the fluid phase and nanoparticles are assumed to be in thermal equilibrium state.
3. Both the fluid and nanoparticles have a constant thermo-physical properties and the density variation is modeled using Boussinesq approximation.
4. Heat generation and viscous dissipation in the fluid are absent.
5. Nanofluids can be treated as a single phase fluid with changed physical parameters such as density, specific heat, thermal conductivity and viscosity in the single phase.
6. No slip occurs between liquid and nanoparticles phases in terms of both temperature and velocity.

The dimensionless forms of the governing equations (continuity, momentum and energy equations) for the present problem can be written as follows (Nasrin and Parvin, 2012):

$$\frac{\partial U}{\partial X} + \frac{\partial V}{\partial Y} = 0 \tag{1}$$

$$U\frac{\partial U}{\partial X} + V\frac{\partial U}{\partial Y} = -\frac{\rho_f}{\rho_{nf}}\frac{\partial P}{\partial X} + Pr\frac{\vartheta_{nf}}{\vartheta_f}\left(\frac{\partial^2 U}{\partial X^2} + \frac{\partial^2 U}{\partial Y^2}\right) \tag{2}$$

$$U\frac{\partial V}{\partial X} + V\frac{\partial V}{\partial Y} = -\frac{\rho_f}{\rho_{nf}}\frac{\partial P}{\partial Y} + Pr\frac{\vartheta_{nf}}{\vartheta_f}\left(\frac{\partial^2 V}{\partial X^2} + \frac{\partial^2 V}{\partial Y^2}\right) + \mathrm{Ra}\,Pr\,\frac{(\rho\beta)_{nf}}{\rho_{nf}\beta_f}\,\theta \tag{3}$$

$$U\frac{\partial \theta}{\partial X} + V\frac{\partial \theta}{\partial Y} = \frac{\alpha_{nf}}{\alpha_f}\left(\frac{\partial^2 \theta}{\partial X^2} + \frac{\partial^2 \theta}{\partial Y^2}\right) \tag{4}$$

Where

$$\theta = \frac{T - T_C}{T_H - T_C}, X = \frac{x}{H}, Y = \frac{y}{H}, U = \frac{u\,H}{\alpha_f}, V = \frac{v\,H}{\alpha_f}, \psi = \frac{\Psi}{\alpha_f}, P = \frac{p\,H^2}{\rho_{nf}\,\alpha_f^2}, Pr = \frac{\vartheta}{\alpha}, and$$

$$\mathrm{Ra} = \frac{g\beta_f(T_H - T_C)H^3}{\vartheta_f\,\alpha_f} \qquad (5)$$

$\alpha_{nf} = k_{nf}/(\rho c_p)_{nf}$ is the thermal diffusivity of nanofluid. The effective density of nanofluid (ρ_{nf}) at reference temperature can be defined as (Nasrin and Parvin, 2012):

$$\rho_{nf} = (1 - \varphi)\rho_f + \varphi\,\rho_s \qquad (6)$$

The heat capacitance of nanofluid can be given as (Nasrin and Parvin, 2012):

$$(\rho c_p)_{nf} = (1 - \varphi)(\rho c_p)_f + \varphi(\rho c_p)_s \qquad (7)$$

Furthermore, the effective thermal expansion coefficient (β_{nf}) and viscosity of nanofluid (μ_{nf}) were introduced by Brinkman (1952) as below:

$$(\rho\beta)_{nf} = (1 - \varphi)(\rho\beta)_f + \varphi(\rho\beta)_s \qquad (8)$$

$$\mu_{nf} = \frac{\mu_f}{(1 - \varphi)^{2.5}} \qquad (9)$$

In addition, the effective thermal conductivity (k_{nf}) of nanofluid is given by Maxwell (1904):

$$\frac{k_{nf}}{k_f} = \frac{k_s + 2k_f - 2\varphi(k_f - k_s)}{k_s + 2k_f + \varphi(k_f - k_s)} \qquad (10)$$

The fluid motion is displayed using the dimensionless stream function (ψ) obtained from velocity components U and V. The relationships between stream function and velocity components for two dimensional flows are:

$$U = \frac{\partial\psi}{\partial Y}, V = -\frac{\partial\psi}{\partial X} \qquad (11)$$

The rate of heat transfer is represented in terms of average Nusselt number at the hot left sidewall ($\overline{Nu}_{\mathrm{h}}$) as follows (Nasrin and Parvin, 2012):

$$\overline{Nu}_{\mathrm{h}} = -\frac{1}{S}\int_0^S \left(\frac{k_{nf}}{k_f}\right)\left[\frac{\partial\theta}{\partial n}\right]_{X=0} dn \qquad (12)$$

Where S and n are the non-dimensional length and coordinate along the inclined heated surface respectively.

2.2 Boundary conditions

On the solid walls no-slip boundary conditions are applied and the relevant non-dimensional boundary conditions of the present problem are expressed as follows**:**

1. The left sidewall of the parallelogrammic cavity is maintained at uniform hot temperature (T_H) so that: $0 \le X \le \cos(\Phi), \theta = 1, V = 0$ and $U = 0$

2. The right sidewall of the parallelogrammic cavity is maintained at uniform cold temperature (T_C) so that: $1 \le X \le 1 + \cos(\Phi), \theta = 0, V = 0$ and $U = 0$

3. The lower and upper horizontal wall of the parallelogrammic cavity is considered adiabatic, so that:

Y=0 and Y=1, $\frac{\partial \theta}{\partial Y} = 0$, U = V = 0

3. Method of solution and verification

The dimensionless continuity, momentum and energy equations (Eqs. (1-4)) are solved numerically with their suitable boundary conditions which are essentially based on the finite volume method (FVM) in addition with hybrid differencing scheme that is used to convert the governing equations to a set of algebraic equations as explained in Patankar (1980). The advantage of the finite volume method is that it provides smooth solutions at the interior domain including the sharp enclosure corners. The parallelogrammic enclosure is meshed utilizing non-uniform grids with a very fine spacing near the enclosure sidewalls by using gird clustering procedure. The iterative solution procedure starts when the computation is initialized by guessing the pressure field. Then, the momentum and energy equations are solved to determine the velocity components and temperature respectively. The pressure is updated using the continuity equation. Even though the continuity equation does not contain any pressure, it can be transformed easily into a pressure correction equation as outlined by Patankar (1980). Equations for the solid and the fluid flow are solved simultaneously as a single domain heat transfer problem. The numerical model is developed in the physical domain, and dimensionless parameters are calculated from the computed velocity and temperature distributions. The iterations are continued until the sum of residuals for all computational cells becomes negligible (less than 10^{-7}) and velocity components do not vary from one iteration to other. In order to examine the influence of grids used in the study on the numerical results, a grid independence test is performed. Eight different sets of meshes are used for the case of Ra=10^6, AR=1, φ=0.2 and Φ =0°. The converged value ($\overline{Nu}_h = 11.921$) is compared with the known values reported by Kahveci (2010) and a very good agreement is satisfied. Therefore, a grid set of (100 x 100) is used in generating all solutions presented in the present work as shown in Fig.2. Moreover, in order to verify the numerical code accuracy, a comparison with the previous published results is necessary. To reach this goal, the present numerical results are verified against the results obtained by the polynomial differential quadrature method published by Kahveci (2010) as shown in Table 2. The comparison of the average Nusselt number at the hot left sidewall is made using the following parameters: Ra = (10^4-10^6), φ = (0-0.2), Φ = 0° and using Cu-Water nanofluid. It is clear from this comparison that the present computed results are in excellent agreement with the corresponding results of Kahveci (2010). This validation gives a good confidence in the current numerical code to deal with present problem.

4. Results and discussion

The flow and thermal fields characteristics in a two-dimensional parallelogrammic enclosure filled with a copper-water nanofluid have been studied and presented in Figures (3-11) for different values of Rayleigh number (Ra), skew angle (Φ) and solid volume fraction (φ) .The Rayleigh number relates the relative magnitude of the viscous and buoyancy forces in the fluid. When buoyancy forces overcome the resistance induced by viscous forces, the natural convection occurs within the parallelogrammic enclosure. Due to the buoyancy force effect, the flow field begins to transfer from the hot left sidewall and then reaches to the insulated top wall. The insulated top wall leads to make the flow field changes its direction and moves towards the cold right sidewall and then changes its direction secondly after hitting the insulated bottom wall. This movement of the flow field creates the usual, regular single circulation vortices which occupies a larger zone of the parallelogrammic enclosure and can be observed in most buoyancy-driven flow problems. For low Rayleigh number (Ra=10^4) as shown in Fig.3, where the heat is transferred mainly due to conduction, the circulation intensity is weak (ψ varies from -1.23 to - 6.52) which reflects a slight flow circulation inside the parallelogrammic enclosure. The figure demonstrates also that the intensity of natural convection circulation increases rapidly as the solid volume fraction and Rayleigh number increase. This behavior is due to the increase of the heat transfer from the hot left sidewall to the nanofluid particles as a result of the velocity increasing. The figure explains also that the hydrodynamic boundary layer thickness increases with the increase of solid volume fraction. As the Rayleigh number increases ($Ra=10^6$) [Fig.5], the vortices change their shape from the uniform circular shape to the non-uniform semi-elliptical shape while the symmetry property of these vortices begin to diminish. Moreover, the circulation intensity increases significantly (ψ varies from -12.11 to - 24.13) as the Rayleigh number increases. Furthermore, the growth of the boundary layer regime increases. This refers that the buoyant flow becomes stronger and the heat transfer is enhanced at high Rayleigh number where convection dominates the flow field. In addition, when the solid volume fraction increases from (5% to 20%), the stream function increases dramatically, for example when ($\Phi=30^o$) it increases about (83 %) and when ($\Phi = -30^o$) it increases about (84.62 %).This increasing when the Rayleigh number is low ($Ra=10^4$). But, when the Rayleigh number is high ($Ra=10^6$), the stream function increases strongly, for example when ($\Phi = 30^o$) it increases about (86.51 %) and when ($\Phi = -30^o$) it increases about (86.81 %).The reason of this significant increasing because as the solid volume fraction increases, the velocity of the nanoparticles increases which causes to increase flow circulation and the thermal energy transport through the fluid. With respect to isotherms, for low Rayleigh number ($Ra=10^4$), [Fig.4] the isotherm lines become approximately vertical in the parallelogrammic enclosure indicating that conduction dominates the heat transfer process. From the other hand, the isotherm lines become irregular, random, approximately horizontal in the middle of the enclosure and greatly deform due to the stronger circulation as the Rayleigh number increases ($Ra=10^6$). This behavior can be clearly seen in Fig.6. As well as, the isotherms begin to accumulate near the hot left and cold right sidewalls of the parallelogrammic enclosure. This is because for high Rayleigh number, natural convection circulation becomes more significant causing the fluid moves more faster and the isotherms begin to accumulate near the enclosure sidewalls. These results cause a clear deformation in isotherm lines and give an indication of the dominating of buoyancy forces at high Rayleigh number. Moreover, as the solid volume fraction increases, the thermal conductivity of nanofluid increases which causes the heat passes much deeper into the nanofluid, before being carried away by the convection currents. This phenomenon leads also to increase the thermal boundary layer thickness. Also, the isotherm lines deflect towards the core of the parallelogrammic enclosure as the solid volume fraction increases. The figures (3-6) depict also the skew angle effect on the streamlines and isotherms in the parallelogrammic enclosure. The skew angle varies as ($\Phi = 0°, 30°, -30°, 60°$ and $-60°$) respectively. It can be observed from figures (3 and 5), that as the skew angle increases in the positive direction from ($\Phi= 0°$ to $\Phi =60°$) or decreases in the negative direction from ($\Phi= 0°$ to $\Phi = -60°$), the stream function decreases. This is due to the reduction of the buoyancy force effect. This behavior can be noticed for all the considered range of Rayleigh number and solid volume fraction. Also , the vortices begin to enlarge towards the upper right and the lower left corners of the parallelogrammic enclosure as the skew angle increases from ($\Phi=30°$) to ($\Phi = 60°$).While, they begin to enlarge towards the upper left and the lower right corners of the parallelogrammic enclosure as the skew angle decreases from ($\Phi=-30°$) to ($\Phi= -60°$).Therefore, it can be concluded that the skew angle can be used to damp the intensity of circulation in the parallelogrammic enclosure for all the considered range of Rayleigh number and solid volume fraction. For this reason, the maximum stream function can be seen when the skew angle is zero ($\Phi= 0°$). With respect to isotherms, it is evident from figures (4 and 6) that as the skew angle increases in the positive direction from ($\Phi= 0°$ to $\Phi= 60°$) or decreases in the negative direction from ($\Phi= 0°$ to $\Phi= -60°$), the shape of isotherm lines becomes approximately similar to the vertical lines indicating that the heat is transferred by conduction. This is due to the reduction in the flow circulation as explained above. From the other side, the isotherm lines are clearly confused when the skew angle is zero ($\Phi=0°$).In this case, the flow circulation role is significant and the heat is transferred by convection. Figures 7 and 8 illustrate respectively the variation of streamlines and isotherms for various aspect ratio (AR) and skew angle (Φ) for pure fluid (φ = 0) and nanofluid (φ = 0.1) when Ra = 10^5. It can be seen that the variation in the aspect ratio from (AR = 0.5) to (AR = 4) causes a clear change in the shape of both streamlines and isotherms. When the aspect ratio is less than one (AR = 0.5) [slender enclosure], the stream function are higher than their corresponding values at another aspect ratio values for both pure fluid and nanofluid. In this case, the convection effect becomes significant and the circulation intensity is strong. This is due to the extension in the enclosure width which increases the flow circulation area and as a result causes to increase the convection effect. It is also observed that when (AR = 0.5), the vortices begin to extend horizontally inside the enclosure taking approximately the ellipsoidal shape. When the aspect ratio is unity (AR=1) [square enclosure], the stream function begins to decrease slightly for both pure fluid and nanofluid. Therefore, it can be concluded that as the aspect ratio increases, the intensity of circulation decreases. This is due to the reduction in the flow circulation area when the aspect ratio increases from (AR = 0.5) to (AR = 1). Also, the core of re-circulating vortices begins to compress inside the enclosure. When the aspect ratio is greater than one (AR = 2 and 4) [shallow enclosure], the stream function begins to decrease rapidly. In this case, the core of re-circulating vortices begins to be more uniform and decreases as the aspect ratio increases. It can be seen in this case that, the convection role becomes slight and the circulation intensity diminishes gradually. This is due to the reduction in the enclosure width which decreases the flow circulation area and as a result causes to damp the convection role. Moreover, the re-circulating vortices inside the enclosure begin to extend vertically and its shape becomes approximately circular. Moreover, it can be noticed in Fig.7, that as the skew angle increases in the positive direction from (Φ= 0° to Φ= 60°) or decreases in the negative direction from (Φ= 0° to Φ= -60°), the stream function decreases due to the decreasing of the buoyancy force effect. From the other side, the flow structure considerably changes and begins to spread along the inclined enclosure sidewalls with changing the skew angle in positive or negative direction for various aspect ratios. With respect to isotherms, the variation in the aspect ratio causes a clear change in the isotherms. When the aspect ratio is less than one (AR = 0.5), a strong disturbance in isotherms can be seen indicating that the heat is transferred by convection. The isotherms are begin to cluster and accumulate adjacent the hot left and the cold right sidewalls and a thermal boundary layer can be observed near these regions. When the aspect ratio is greater than one (AR = 2 and 4), the isotherms are approximately linear in shape and nearly parallel one to each other. This refers that the heat is transferred by conduction due to the flow circulation decreasing. Furthermore, it can be noticed from Fig.8 that the isotherms for the nanofluid are more vertical than the pure water indicating a high conduction heat transfer contribution. This is because the addition of nanofluid with higher thermal conductivity improves significantly the conduction heat transfer effect. Fig. 9 explains the variation of the average Nusselt number at the hot left sidewall with skew angle for φ = 0 and 0.1, AR=1 and Ra = 10^4, 10^5 and 10^6 respectively. It can be seen that the average Nusselt number increases as the Rayleigh number increases. This is due to the increase in the convection circulation intensity as a result of high buoyancy forces. From the other side, the average Nusselt number increases also with the addition of nanofluid (φ=0.1) compared with its value of pure fluid (φ = 0) for all values of skew angle and Rayleigh number. The reason of this behavior is due to the strong circulation produced by the thermal energy transport with the addition of nanofluid which accelerates the flow. Also, the effective thermal conductivity increases with the addition of nanofluid which eventually leads to enhance the heat transfer rate represented by the average Nusselt number. Fig.9 shows also, that the maximum value of the average Nusselt number can be obtained when the skew angle equals zero. This result can be seen for all values of Rayleigh number and solid volume fraction. This is due to the high amount of the flow velocity when the skew angle equals zero. But, when the skew angle increases in the positive direction from (Φ= 0° to Φ= 60°) or decreases in the negative direction from (Φ= 0° to Φ= -60°), the average Nusselt number begins to decrease due to the reduction in the flow velocity which causes to reduce the transport of thermal energy through the fluid causing a clear reduction in the value of average Nusselt number. Again, this behavior can be noticed for all values of solid volume fraction and Rayleigh number. Fig.10 shows the variation of the average Nusselt number with aspect ratio for various skew angle at Ra $=10^5$ and φ = 0, 0.1. Again, it can be seen that the average Nusselt number is maximum for both pure fluid and nanofluid when the skew angle equals zero. After that, it begins to decrease when the skew angle increases in the positive direction or decreases in the negative direction for the same reasons explained previously. In addition, the average Nusselt number increases with the addition of nanofluid (φ = 0.1) compared with its value of pure fluid (φ = 0) for all values of skew angle and aspect ratio. The reasons will be discussed later. In general, it is clear from Fig.10, that there is a linear variation between the average Nusselt number and the aspect ratio and no remarkable increase of the average Nusselt number can be observed when the aspect ratio increases. This behavior can be seen when the skew angle (Φ= 0° and Φ= $\mp$30°). The maximum value of the average Nusselt number occurs adjacent (AR = 2).When the aspect ratio is less than (AR = 2) , or greater than (AR= 2) the average Nusselt number decreases due to the reduction in the convection effect and the flow circulation area respectively. In contrast of this general behavior, when the aspect ratio is greater than (AR = 2) for (Φ= $\mp$60°), the average Nusselt number increases continuously when the aspect ratio increases. This is because at high values of skew angle (Φ= $\mp$60°) the strong reduction in the convection role causes a high increase of the conduction role in the heat transfer process which causes a jump in the average Nusselt number values. This behavior can be seen for both fluid and nanofluid. However, it can be noticed also from Fig.10, that the maximum value of the average Nusselt number occurs adjacent (AR = 2). Finally, Fig.11 demonstrates the variation of average Nusselt number along the hot left sidewall with Rayleigh number for various values of solid volume fraction and skew angle and AR=1.It can be observed that as the Rayleigh number and solid volume fraction increase , the average Nusselt number increases as a result of strong flow circulation , the increase in the buoyancy force effect when the Rayleigh number increases and the increase in the effective thermal conductivity and flow velocity when the solid volume fraction increases. Also it is interesting to see, that the average Nusselt number along the hot left sidewall decreases as the skew angle increases in the positive direction from (Φ= 0° to Φ= 60°) or decreases in the negative direction from (Φ= 0° to Φ= -60°) for the same reasons explained previously. Furthermore, for all values of the skew angle and the Rayleigh number, the maximum Nusselt number can be obtained when the solid volume fraction is high (φ=0.2) while the minimum Nusselt number can be obtained for pure fluid (φ = 0).This result indicates that the addition of nanofluid enhances significantly the heat transfer performance.

5. Conclusions

The following conclusions can be drawn from the results of the present work:

1-When the solid volume fraction increases, the intensity of the circulation increases as a result of high energy transport through the flow related with the irregular and random movement of the nanoparticles. Streamlines strength also increases with increasing the volume fraction of nanoparticles.

2-When the solid volume fraction and Rayleigh number increase, the flow stream function increases strongly, for example when ($\Phi = 30^o$) it increases about (86.51 %) and when ($\Phi = -30^o$) it increases about (88.81 %).

3-The results indicate that as the Rayleigh number increases, a high heat transfer rate can be observed for all values of solid volume fraction. This is due to increase the buoyancy force effect.

4-When the solid volume fraction increases, the thermal and hydrodynamic boundary layer thickness increase and the isotherm lines begin to accumulate adjacent the enclosure sidewalls which refer that a large temperature gradient exists there.

5-The stream function decreases when the skew angle increases in the positive direction from (Φ= 0° to Φ= 60°) for all the considered range of Rayleigh number and solid volume fraction. The same behavior can be observed when the skew angle decreases in the negative direction from (Φ = 0° to Φ= -60°).

6- The size and strength of circulation vortices increase when the skew angle increases in the negative direction greater than corresponding values in the negative direction.

7-When the skew angle increases in the positive direction from (Φ= 0° to Φ= 60°) or decreases in the negative direction from (Φ=0° to Φ= -60°), the isotherm lines are symmetrical in shape, and parallel to the enclosure hot and cold sidewalls where the thermal energy is transferred by conduction. At skew angle equals zero, a clear confusion can be seen in the isotherms indicating that the convection effect is significant.

8-The average Nusselt number at the hot left sidewall increases with the addition of the nanofluid and increasing the Rayleigh number.

9-The average Nusselt number at the hot left sidewall has maximum value when the skew angle equals zero. But, it begins to decrease gradually as the skew angle increases in the positive direction or decreases in the negative direction.

10-The variation in the enclosure aspect ratio causes a strong change on the flow and the thermal fields inside the parallelogrammic enclosure.

11-When the enclosure aspect ratio is less than one (AR = 0.5), the convection effect becomes strong and the circulation strength increases for both pure fluid and nanofluid. A reverse behavior can be seen when the aspect ratio is greater than one (AR = 2 and 4).

12-When the skew angle (Φ= 0° and Φ= $\mp$30°), the aspect ratio does not have a significant effect on the average Nusselt number at the hot left sidewall. But, when the aspect ratio is greater than (AR = 2) for (Φ= $\mp$60°), the average Nusselt number increases continuously when the aspect ratio increases.

References

Abu-Nada, E., Masoud, Z., Oztop, H. and Campo, A., 2010. Effect of nanofluid variable properties on natural convection in enclosures, Int. J. of Thermal Sci. 49, 479–491.

Abu-Nada, E. and Oztop, H., 2009. Effects of inclination angle on natural convection in enclosures filled with Cu-water nanofluid, Int. J. of Heat and Fluid Flow 30, 669–678.

Akbari, M., Behzadmehr, A. and Shahraki, F., 2008. Fully developed mixed convection in horizontal and inclined tubes with uniform heat flux using nanofluid, Int. J. of Heat and Fluid Flow 29, 545–556.

Aldridge, K. and Yao, H., 2001. Flow features of natural convection in a parallelogrammic enclosure, Int. Comm. in Heat and Mass Transfer 28 (7) 923–931.

Alloui, Z., Vasseur, P. and Reggio, M., 2012. Natural convection of nanofluids in a shallow cavity heated from below, To be submitted to Int. J. of Thermal Sci..

Aminossadati, S. and Ghasemi, B., 2009. Natural convection cooling of a localized heat source at the bottom of a nanofluid-filled enclosure, European Journal of Mechanics B/Fluids 28, 630–640.

Anilkumar, S. and Jilani, G., 2009. Convective heat transfer enhancement in an enclosure with fin utilizing nanofluids, Int. J. of Mechanical, Industrial and Aerospace Engineering 3(2), 104–111.

Anoop, K., Sundararajan, T. and Das, S., 2009. Effect of particle size on the convective heat transfer in nanofluid in the developing region, Int. J. of Heat and Mass Transfer 52, 2189–2195.

Baïri, A., 2008. On the Nusselt number definition adapted to natural convection in parallelogrammic cavities, Applied Thermal Engineering 28, 1267–1271.

Brinkman, H., 1952.The viscosity of concentrated suspensions and solution, J. of Chemical and Physics 20, 571-581.

Chung, K. and Trefethen, L., 1982. Natural convection in a vertical stack of inclined parallelogrammic cavities, Int. J. of Heat and Mass Transfer 25(2), 277–284.

Corcione, M., 2010. Heat transfer features of buoyancy-driven nanofluids inside rectangular enclosures differentially heated at the sidewalls, Int. J. of Thermal Sci. 49, 1536–1546.

Daungthongsuk, W. and Wongwises, S., 2007. A critical review of convective heat transfer nanofluids, Renewable and Sustainable Energy Reviews 11,797–817.

Elgafy, A. and Lafdi, K., 2007. Engineering solution in monitoring nanoparticle-fluid flow during nanocomposites processing, J. of Nanoparticle Research 9, 441–454.

Ghasemi, B. and Aminossadati, S., 2009. Natural convection heat transfer in an inclined enclosure filled with a water-Cuo nanofluid, Numerical Heat Transfer Part A 55(8), 807–823.

Ghasemi, B. and Aminossadati, S., 2010. Periodic natural convection in a nanofluid-filled enclosure with oscillating heat flux, Int. J. of Thermal Sci. 49,1–9.

Ho, C. and Lin, C., 2006. Experiments on natural convection heat transfer of a nanofluid in a square enclosure, Proceedings of the 13th International Heat Transfer Conference, Sydney, Australia.

Ho, C., Chen, M. and Li, Z., 2008. Numerical simulation of natural convection of nanofluid in a square enclosure: effects due to uncertainties of viscosity and thermal conductivity, Int. J. of Heat and Mass Transfer 51, 4506–4516.

Ho, C., Liu, W. , Chang, Y. and Lin, C., 2010. Natural convection heat transfer of alumina-water nanofluid in vertical square enclosures: An experimental study, Int. J. of Thermal Sci. 49, 1345–1353.

Hwang, K., Lee, J. and Jang, J., 2007. Buoyancy-driven heat transfer of water-based Al_2O_3 nanofluids in a rectangular cavity, Int. J. of Heat and Mass Transfer 50, 4003–4010.

Hyun, J. and Choi, B., 1990. Transient natural convection in a parallelogram-shaped enclosure, Int. J. of Heat and Fluid Flow 11 (2), 129–134.

Jou, R. and Tzeng, S., 2006. Numerical research of nature convective heat transfer enhancement filled with nanofluids in a rectangular enclosure, Int. Comm. in Heat and Mass Transfer 33, 727–736.

Kahveci, K., 2010. Buoyancy driven heat transfer of nanofluids in a tilted enclosure, ASME Journal of Heat Transfer 132, 529-541.

Keblinski, P., Phillpot, S. ,Choi, S. and Eastman, J., 2002. Mechanisms of heat flow in suspensions of nano-sized particles (nanofluids), Int. J. of Heat and Mass Transfer 45, 855-863.

Khanafer, K., Vafai, K. and Lightstone, M., 2003. Buoyancy-driven heat transfer enhancement in a two-dimensional enclosure utilizing nanofluids, Int. J. of Heat and Mass Transfer 46, 3639-3653.

Lin, K. and Violi, A., 2010. Natural convection heat transfer of nanofluids in a vertical cavity: Effects of non-uniform particle diameter and temperature on thermal conductivity, Int. J. of Heat and Fluid Flow 31, 236–245.

Maekawa, T. and Tanasawa, I., 1982. Natural Convection heat transfer in parallelogrammic enclosures, Proceeding of the Seventh International Heat Transfer Conference ,Vol. 2, Munchen, pp: 227-233.

Mahmoudi, A., Shahi, M., Raouf, A. and Ghasemian, A., 2010.Numerical study of natural convection cooling of horizontal heat source mounted in a square cavity filled with nanofluid, Int. Comm. in Heat and Mass Transfer 37,1135–1141.

Maxwell, J., 1904. A treatise on electricity and magnetism, Second Edition, Oxford University Press, Cambridge.

Nasrin, R., and Parvin, S., 2012. Investigation of buoyancy-driven flow and heat transfer in a trapezoidal cavity filled with water–Cu nanofluid, Int. Comm. in Heat and Mass Transfer 39, 270–274.

Oztop, H. and Abu-Nada, E., 2008. Numerical study of natural convection in partially heated rectangular enclosures filled with nanofluids, Int. J. of Heat and Fluid Flow 29,1326–1336.

Patankar, S., 1980. Numerical heat transfer and fluid flow, Hemisphere Publishing Corporation, New York.

Saleh, H., Basriati, S. and Hashim, I., 2011, Solutions of natural convection of nanofluids in a parallelogrammic enclosure by finite difference method, Journal of Matematika Dan Sains 16(2) 77-81.

Santra, A., Sen, S. and Chakraborty, N., 2008. Study of heat transfer in a differentially heated square cavity using copper–water nanofluid, Int. J. of Thermal Sci. 48, 1113–1122.

Santra, A., Sen, S. and Chakraborty, N., 2009. Study of heat transfer due to laminar flow of copper–water nanofluid through two isothermally heated parallel plates, Int. J. of Thermal Sci. 48, 391–400.

Seki, N., Fokosako, S. and Yamaqushi, A., 1983.An experimental study of free convective heat transfer in a parallelogrammic enclosure, ASME J. of Heat Transfer 105, 433-439.

Trisaksri, V. and Wongwises, S., 2007. Critical review of heat transfer characteristics of nanofluids, Renewable and Sustainable Energy Reviews 11, 512–523.

Wang, X. and Mujumdar, A., 2007. Heat transfer characteristics of nanofluids: a review, Int. J. of Thermal Sci. 46, 1–19.

Table (1) Thermophysical properties of base fluid (water) and nanoparticles (Cu) [Abu-Nada and Oztop , 2009].

Physical properties	Fluid phase (Water)	Cu
c_p (J/kg.K)	4179	385
ρ (kg/m^3)	997.1	8933
k (W/m.K)	0.613	400
$\alpha \times 10^7 (m^2/s)$	1.47	1163.1
$\beta \times 10^5 (1/K)$	21	1.67

Table (2) Comparison of the average Nusselt number at the left hot sidewall with those of previous study of Kahveci (2010) for validation of the present numerical code.

	Kahveci (2010)	Present work	Kahveci (2010)	Present work	Kahveci (2010)	Present work	Maximum error
φ \ Ra	10^4	10^4	10^5	10^5	10^6	10^6	
0.00	2.274	2.271	4.722	4.719	9.230	9.224	-0.065
0.05	2.421	2.428	5.066	5.093	9.962	9.954	0.523
0.10	2.553	2.554	5.384	5.383	10.656	10.654	-0.018
0.15	2.670	2.667	5.674	5.673	11.310	11.299	-0.112
0.20	2.776	2.774	5.937	5.935	11.921	11.906	-0.125

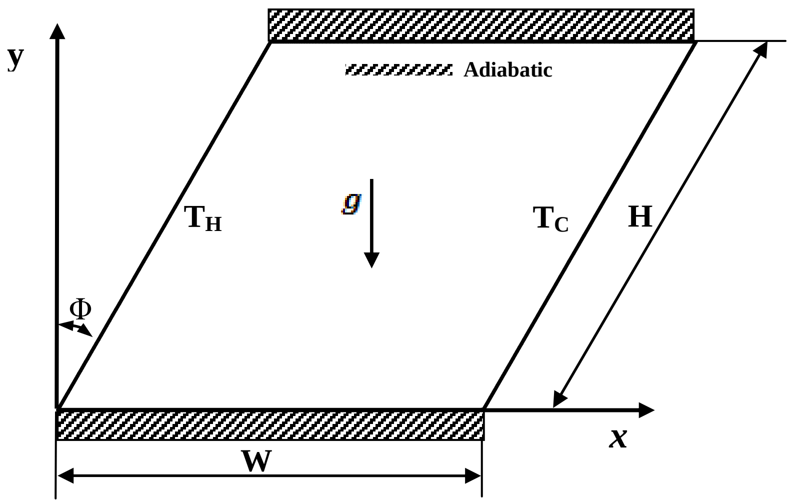

Fig. 1. Schematic diagram and coordinate system of the physical domain with boundary conditions.

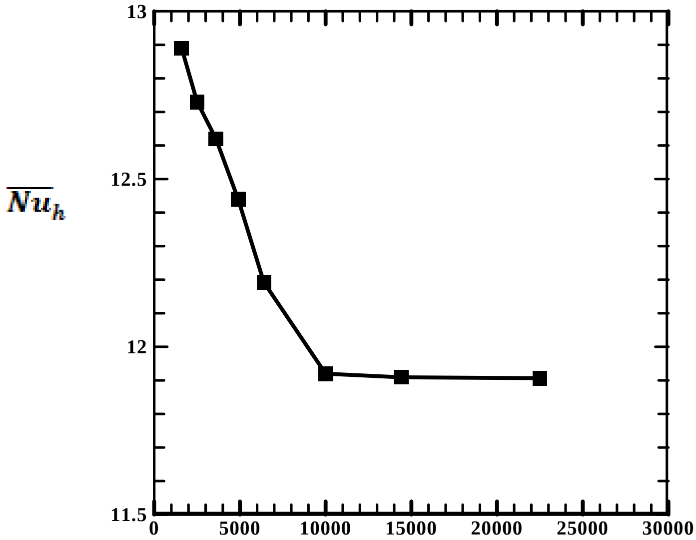

Fig. 2. Convergence of average Nusselt number along the hot left side wall with grid refinement at Ra=10^6, φ = 0.2, AR=1 and Φ = 0°.

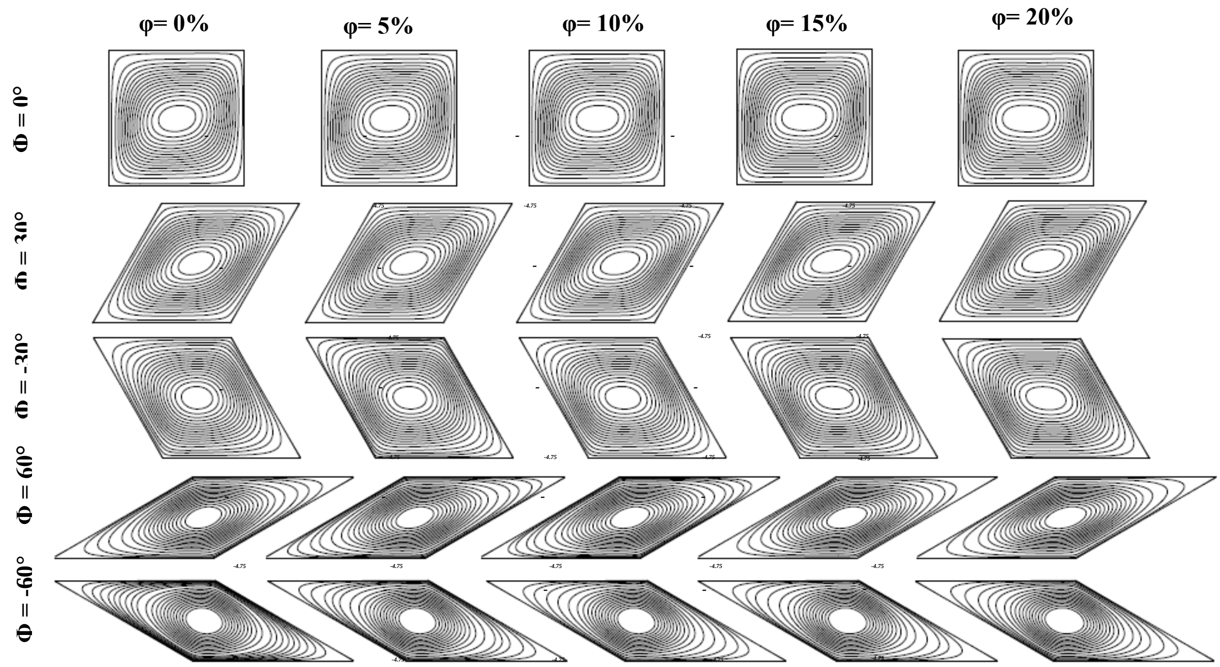

Fig. 3. Variation of streamlines for different solid void fractions (φ) and skew angles (Φ**)**

Ra = 10^4

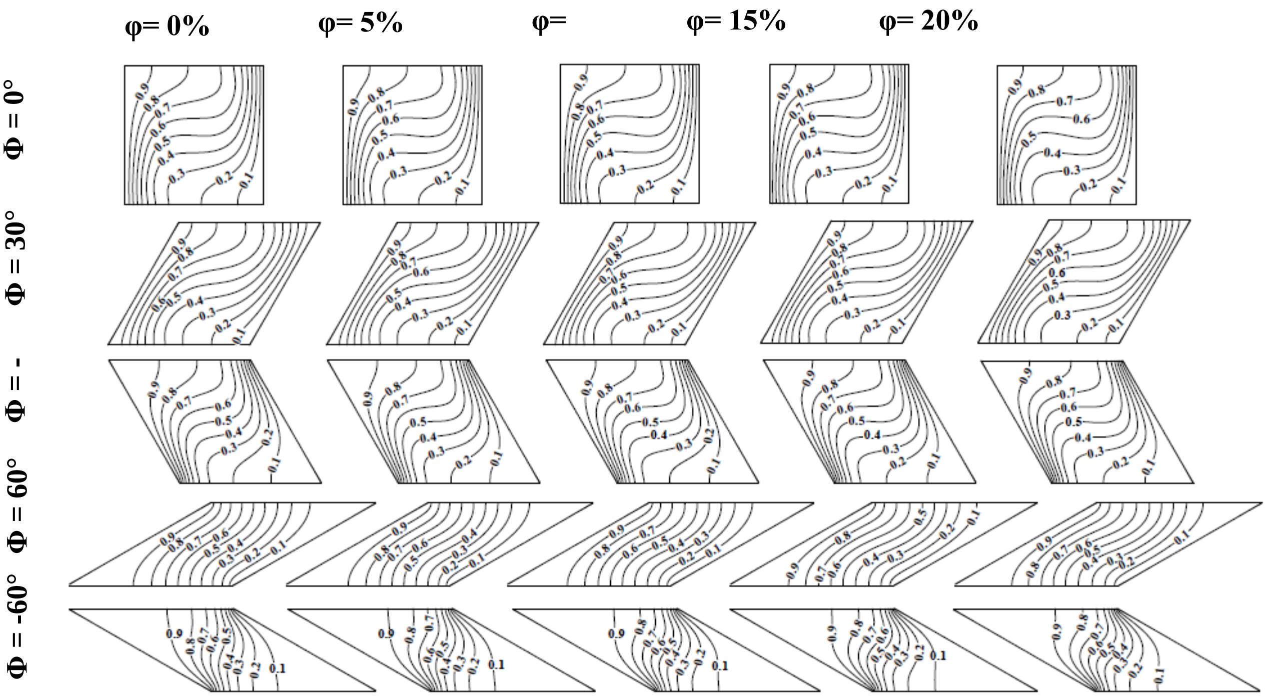

Fig. 4. Variation of isotherms for different solid void fractions (φ) and skew angles (Φ)

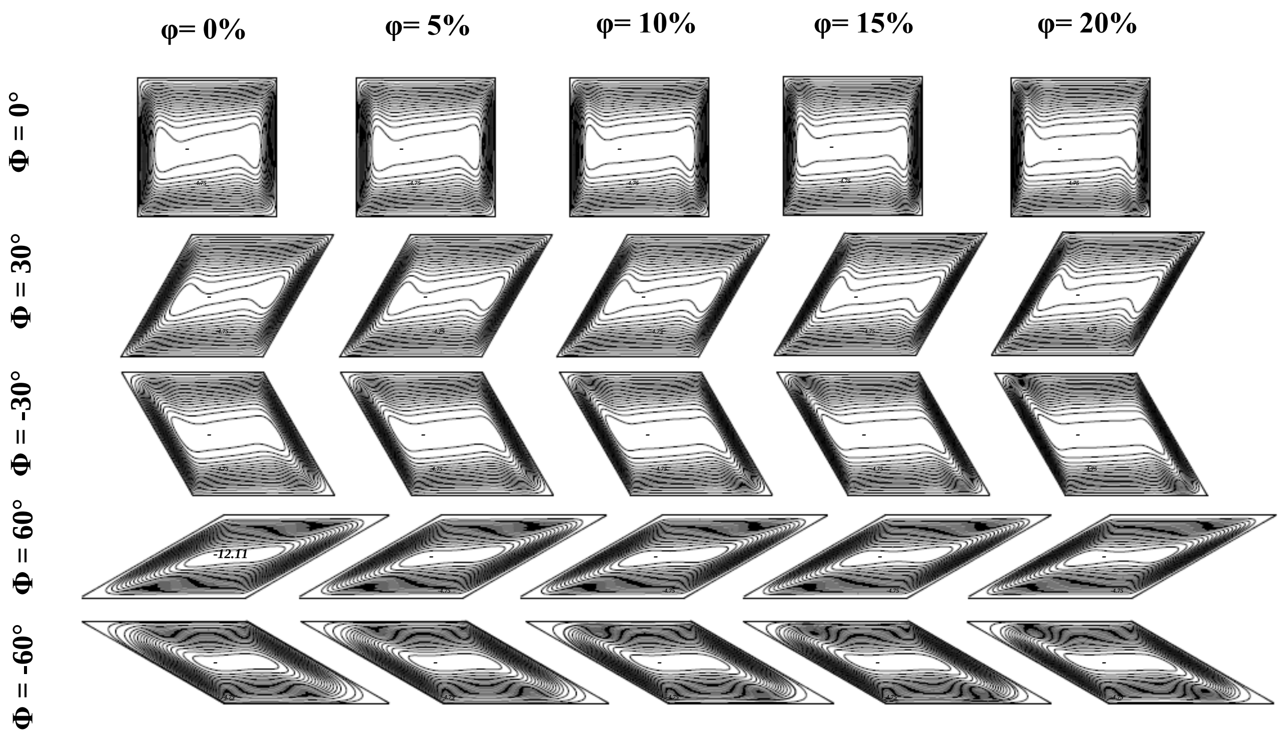

Fig. 5. Variation of streamlines for different solid void fractions (φ) and skew angles (Φ) at Ra= 10^6.

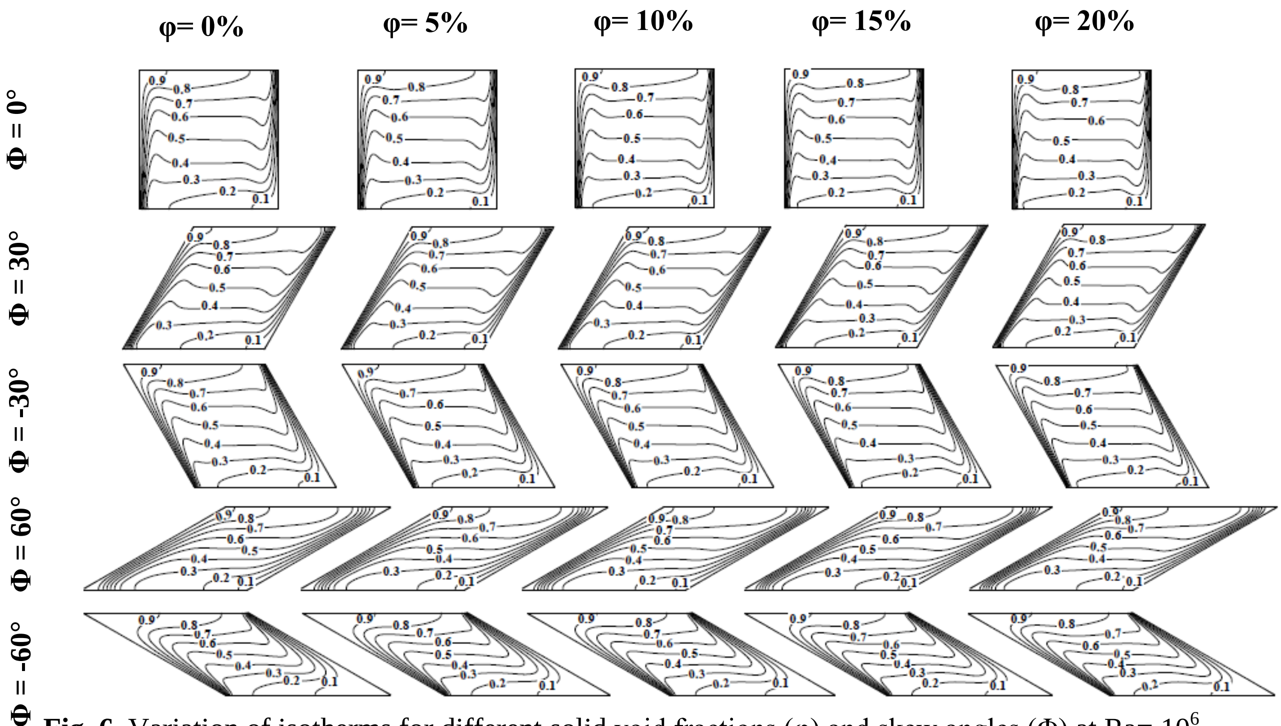

Fig. 6. Variation of isotherms for different solid void fractions (φ) and skew angles (Φ) at Ra= 10^6.

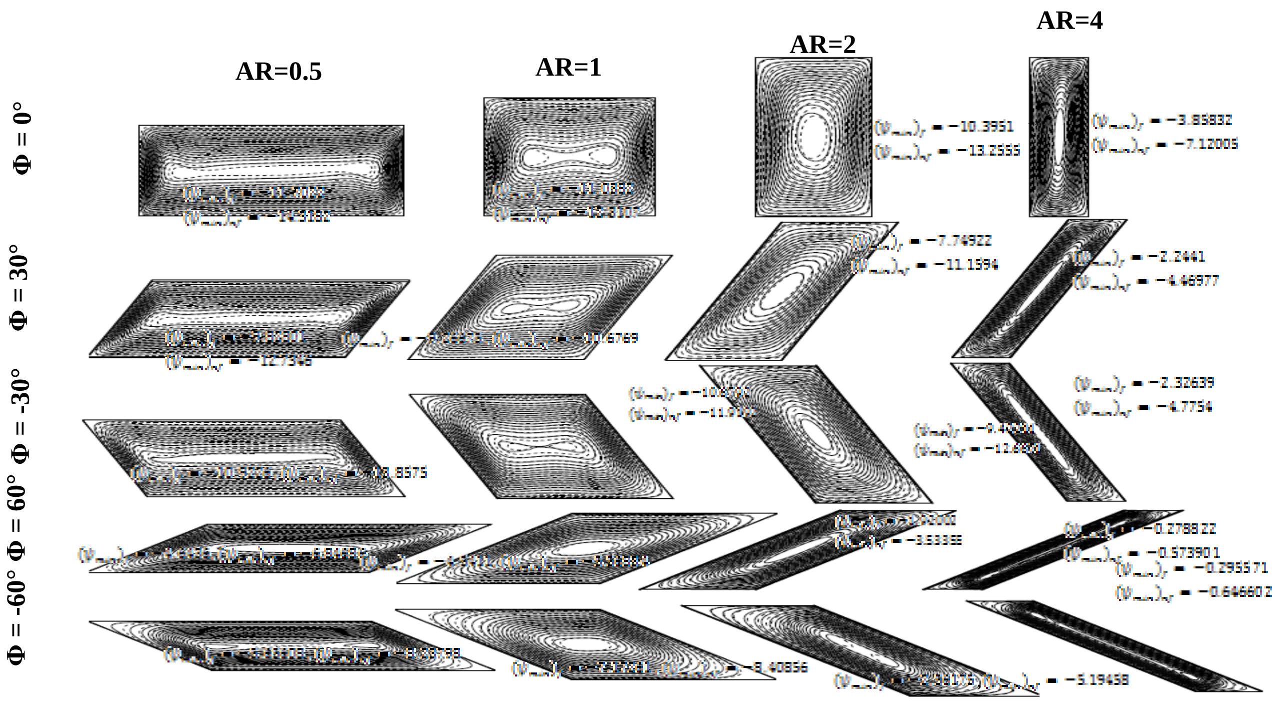

Fig. 7. Variation of streamlines for various aspect ratios (AR) and skew angles (Φ**)** at Ra= 10^5, **φ= 0, 0.1** with pure fluid (dashed lines ---) and nonofluid (solid lines ——).

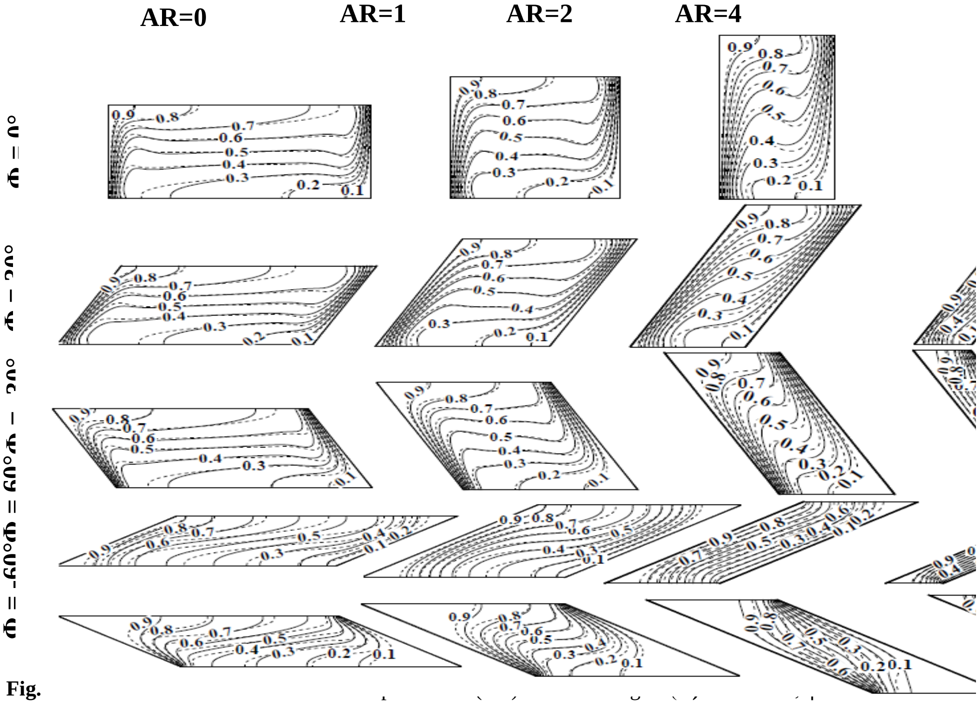

Fig.

0, 0.1 with pure fluid (dashed lines ---) and nonofluid (solid lines ____).

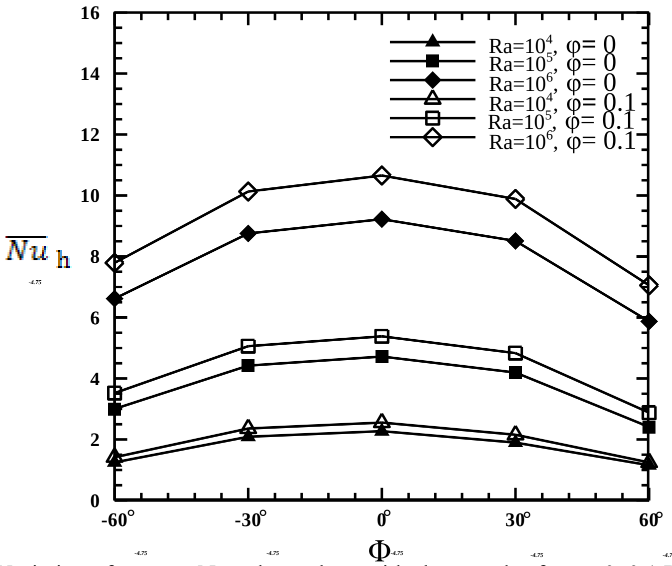

Fig.9 Variation of average Nusselt numbers with skew angles for φ= 0, 0.1 Ra=10^4&$10^6$and AR=1.

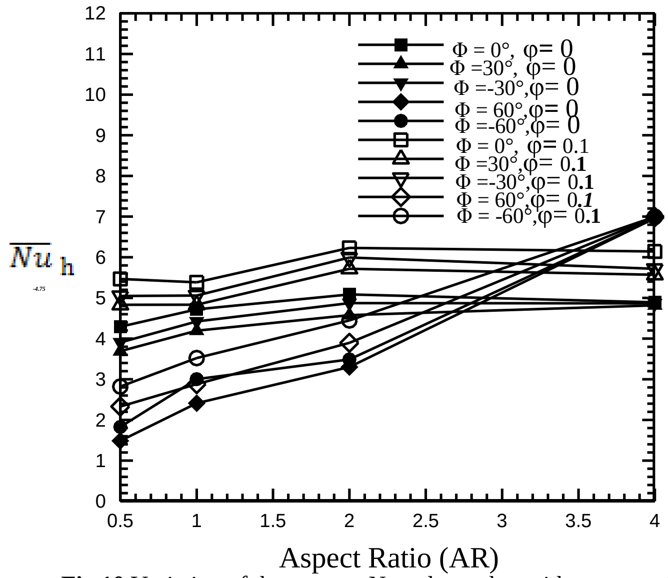

Fig.10 Variation of the average Nusselt number with aspect ratio for various skew angles at Ra=10^5 and φ= 0, 0.1.

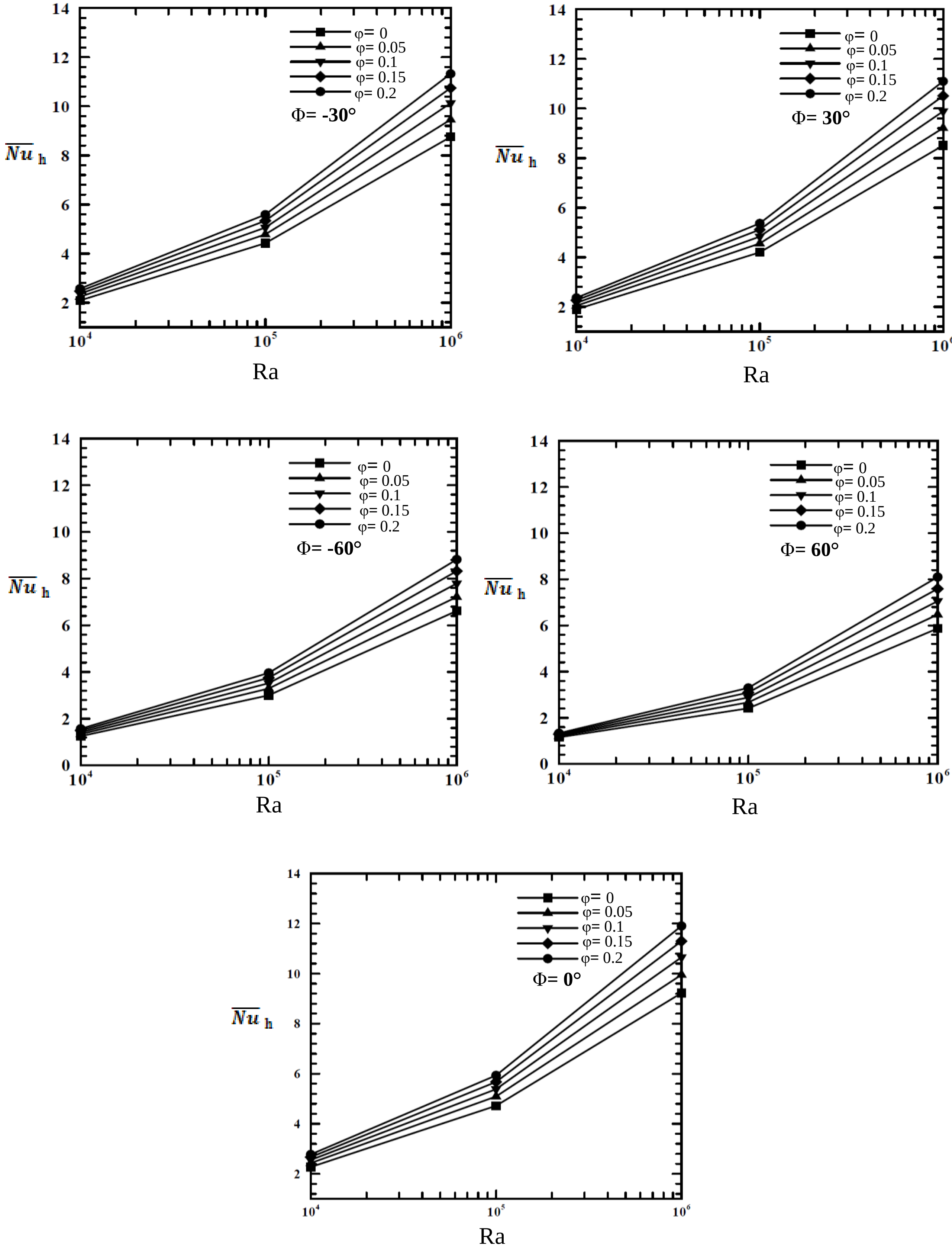

Fig.11. Variation of average Nusselt numbers along the left hot sidewall with Rayleigh numbers for various values of volume fraction and skew angle at AR=1.